



HAL
open science

Detailed Modeling and Evaluation of the Potential Impact of Blue Jet on the Atmospheric Chemistry

C. Xu, Nathalie Huret, S. Celestin, X. Qie

► **To cite this version:**

C. Xu, Nathalie Huret, S. Celestin, X. Qie. Detailed Modeling and Evaluation of the Potential Impact of Blue Jet on the Atmospheric Chemistry. *Journal of Geophysical Research: Atmospheres*, 2023, 128, 10.1029/2023JD038668 . insu-04379377

HAL Id: insu-04379377

<https://insu.hal.science/insu-04379377v1>

Submitted on 8 Jan 2024

HAL is a multi-disciplinary open access archive for the deposit and dissemination of scientific research documents, whether they are published or not. The documents may come from teaching and research institutions in France or abroad, or from public or private research centers.

L'archive ouverte pluridisciplinaire **HAL**, est destinée au dépôt et à la diffusion de documents scientifiques de niveau recherche, publiés ou non, émanant des établissements d'enseignement et de recherche français ou étrangers, des laboratoires publics ou privés.

JGR Atmospheres

RESEARCH ARTICLE

10.1029/2023JD038668

Key Points:

- Ozone enhanced in the middle stratosphere by the impact of blue jet (BJ) discharge during the first 100 s
- Ozone depletion appears in the middle and upper stratosphere after 48 hr of BJ discharge, and the ozone layer “shifts” to a lower altitude
- The enhancement of chlorine and bromine reservoirs can be transported over long distances and be reactivated later to destroy ozone

Correspondence to:

N. Huret,
n.huret@opgc.fr





Citation:

Xu, C., Huret, N., Celestin, S., & Qie, X. (2023). Detailed modeling and evaluation of the potential impact of blue jet on the atmospheric chemistry. *Journal of Geophysical Research: Atmospheres*, 128, e2023JD038668. <https://doi.org/10.1029/2023JD038668>

Received 7 FEB 2023

Accepted 28 OCT 2023

Detailed Modeling and Evaluation of the Potential Impact of Blue Jet on the Atmospheric Chemistry

C. Xu¹ , N. Huret² , S. Celestin³ , and X. Qie^{1,4} 

¹Key Laboratory of Middle Atmosphere and Global Environment Observation (LAGEO), Institute of Atmospheric Physics, Chinese Academy of Sciences, Beijing, China, ²LaMP/OPGC, CNRS, Université Clermont Auvergne, Clermont-Ferrand, France, ³LPC2E, CNRS, Université d'Orléans, Orléans, France, ⁴College of Earth and Planetary Science, University of Chinese Academy of Sciences, Beijing, China

Abstract To evaluate the impact of a blue jet (BJ) discharge on the chemical system in the whole stratosphere as a function of altitude, we developed a detailed ion-neutral chemistry model. The BJ discharge is formed as a streamer discharge up to 50 km with a leader part up to 28 km associated with high-temperature chemistry. The simulations are performed in a 2-day duration to investigate diurnal variations of chemical perturbations at the altitudes of every 2 km from 20 to 50 km. The specific chemistry processes during the leader (considering the molecular diffusion) and streamer discharges react with the whole stratospheric chemical families (oxygen, nitrogen, chlorine, and bromine). We systematically compare the simulations with and without the BJ discharge. The results obtained during the first 100 s indicate the ozone enhanced in the middle stratosphere, while no obvious change in the lower and close to the top of the stratosphere. After 2 days, simulations show that the entire neutral chemical stratospheric system is modified with the enhancement of nitrogen oxides, chlorine, and bromine reservoirs. As a consequence, ozone depletion appears in the middle and upper stratosphere due to the catalytic cycle associated with reactive NO_x ($=\text{NO} + \text{NO}_2$). Each chemical family results in a new equilibrium, and the ozone layer appears to be “shifted” to a lower altitude with its maximum less abundance. Due to the long lifetimes of the chlorine and bromine reservoirs in the stratosphere, the chemical perturbations caused by the BJ discharge at all studied altitudes are maintained.

Plain Language Summary Blue jet (BJ) is a type of upper atmospheric discharge which produces nitrogen oxides ($\text{NO}_x = \text{NO} + \text{NO}_2$) through the same chemical reactions as the tropospheric discharges. As stratospheric NO_x contributes to ozone depletion and BJ occurs at the altitude of the stratospheric ozone layer, this study estimates its chemical effects in the stratosphere using a detailed plasma-chemistry model, focusing on the chemical families of oxygen, nitrogen, chlorine, and bromine. Results show that ozone in the mid-stratosphere increases during the first 100 s, but there are no significant changes in the lower or upper stratosphere. However, after 2 days of simulation, BJ causes changes in nitrogen oxides, chlorine, and bromine that results in ozone depletion in the middle and upper stratosphere. The changes in the chemical system persist as the chemicals involved have long lifetimes in the stratosphere. The ozone layer also shifts to a lower altitude with less abundance. This study explores the chemical effect of transient luminous events at higher altitudes.

1. Introduction

The ozone (O_3) layer exists in the stratosphere between a height of ~ 10 – 50 km with its maximum concentration in the middle stratosphere in the altitude range of 15–35 km above the Earth's surface. The existing stratospheric O_3 layer is an important component of the chemical equilibrium of the atmosphere, which plays a key role in modulating the vertical temperature gradient in the stratosphere, given that O_3 efficiently absorbs solar energy, protecting the biosphere from absorbing harmful ultraviolet solar radiation (wavelengths shorter than 340 nm). The photochemical production of stratospheric O_3 modulates the solar radiative forcing of climate (Haigh, 1994). Stratospheric ozone thus impacts global climate through atmospheric radiative budget processes and chemical equilibrium. Blue jet (BJ) is one of the transient luminous events (e.g., Chuang & Chen, 2022; Li et al., 2023; Tomicic et al., 2023; Xu et al., 2023; Yang et al., 2020), which occurring at the altitude of the stratospheric ozone layer, therefore, the chemical impact of BJs on stratospheric chemistry is important. The physical structure of BJ includes the streamer zone and a leader channel (e.g., Raizer et al., 2010). BJ streamers impact atmospheric chemistry by generating an electric field that drives electron impact on air molecules and atoms by ionization, dissociation, and excitation processes (Goldenbaum & Dickerson, 1993), while the BJ leader with high gas temperature

mainly does so through thermal ionization and thermal decomposition (e.g., Aleksandrov et al., 1997; Winkler & Notholt, 2015).

The chemical impacts of BJ streamer in the stratosphere have been estimated by various model studies (Gordillo-Vázquez & Pérez-Invernón, 2021; Mishin, 1997; Pérez-Invernón et al., 2019; Smirnova et al., 2003; Winkler & Notholt, 2015; Xu et al., 2020), but they are still not fully understood. Compare to the model studies of Mishin (1997), Smirnova et al. (2003), and Winkler and Notholt (2015), Xu et al. (2020) developed a detailed plasma chemistry model for representing the BJ streamer, which used the realistic reduced electric field and performed the simulation over several days. Xu et al. (2020) only revealed the chemical impact of BJ streamer at 27 km, and did not consider the impact of BJ leader and these impacts on the whole stratospheric profile. Winkler and Notholt (2015) did a model study on the chemical impact of BJ leader. Although they displayed the leader impact at the altitudes from 18 to 27 km, the chemical evolutions were stopped at 0.5 s after the leader discharge, whereas the perturbed chemical species by BJ leader could impact the atmospheric chemistry in a longer time than a few seconds. Moreover, their study did not fully account for the chemical species of the chlorine and bromine family, which are known to play a significant role in ozone depletion (Portmann et al., 2012). Pérez-Invernón et al. (2019) estimated the global-scale stratospheric chemical effects of BJ. Their study provided the impact of BJ events at global scale using a chemistry-climate model (Whole Atmosphere Community Climate Model) that used the BJ streamer and leader predictions of the model of Winkler and Notholt (2015) as input concentrations. Pérez-Invernón et al. (2019) highlighted a significant enhancement of N_2O density and a slight (5%) depletion of ozone in the stratosphere due to BJ chemical activity after considering the difference in the ozone annual average density between two simulations of 10 years with and without BJ. Therefore, the chemical impact of BJ at a long-term scale (e.g., 2 days to investigate diurnal variations of chemical perturbations) should be evaluated using a more detailed chemical model with realistic parameterization of streamer and the impact of chlorine and bromine species.

The objective of this study is to investigate the chemical processes associated with BJ streamers and leaders as a function of altitude from 20 to 50 km, especially the O_3 chemistry process. Portmann et al. (2012) reported that between the altitudes of 18–22 km, O_3 depletion is governed first by the HO_x ($=OH + HO_2$) cycle and second by the NO_x cycle. The NO_x cycle represents a major sink for O_3 in the middle stratosphere (from 22 to 43 km). It is evident that the cycles of HO_x and ClO_x ($=Cl + ClO$)/ BrO_x ($=Br + BrO$) are dominant in the upper stratosphere (higher than 43 km). Moreover, nitrous oxide (N_2O) is an important greenhouse gas that can contribute to ozone deplete, and it could be measured using instruments such as Aura-Microwave Limb Sounder (MLS). To investigate the variation of N_2O , it is better to understand the impacted chemical processes by BJ, and simulation results could be validated with the measured data. Thus, this study focuses on the chemical species associated with O_3 chemistry, like nitric oxide, and the chemical families of chlorine, bromine and hydrogen, and N_2O .

To investigate the BJ discharge from 20 to 50 km, it is necessary to consider streamer discharge as well as the leader channel up to 28 km (Da Silva & Pasko, 2013) with the diffusion effect of chemical species. In this study, we first present the Microphysical Photochemical Ozone-Streamer (MiPO-Streamer) model with its realistic streamer parameterization generalized from 20 km up to 50 km, and develop the MiPO-Leader model for the leader at altitudes between 20 and 30 km as well as taking into account the diffusion of the produced species during the leader phase. Then, performing two sets of simulations with and without BJ discharge by considering the impact of the leader channel at the low stratosphere, we investigate the chemical impact of BJ on ozone volume mixing ratio (VMR) as a function of altitude just after the discharge and during the two diurnal variations. In the last part, we analyze in detail the budget of the stratospheric major chemical families associated with ozone (nitrogen, chlorine, and bromine) and nitrous oxide to explore the perturbation in the entire chemical system and the chemical signal that exists during two diurnal variations and could subsist later.

2. Model Description

2.1. MiPO-Streamer Model Description

The MiPO-Streamer model is a plasma chemistry box model that considers 118 species and 1,760 reactions (Xu et al., 2020). The core of this model has been widely used over the last 20 years to interpret balloon and satellite measurements associated with stratospheric ozone (e.g., Brogniez et al., 2003; Croizé et al., 2015; Grossel et al., 2010; Huret et al., 2003; Rivière et al., 2000, 2002). It considers oxygen, hydrogen, nitrogen, chlorine, and

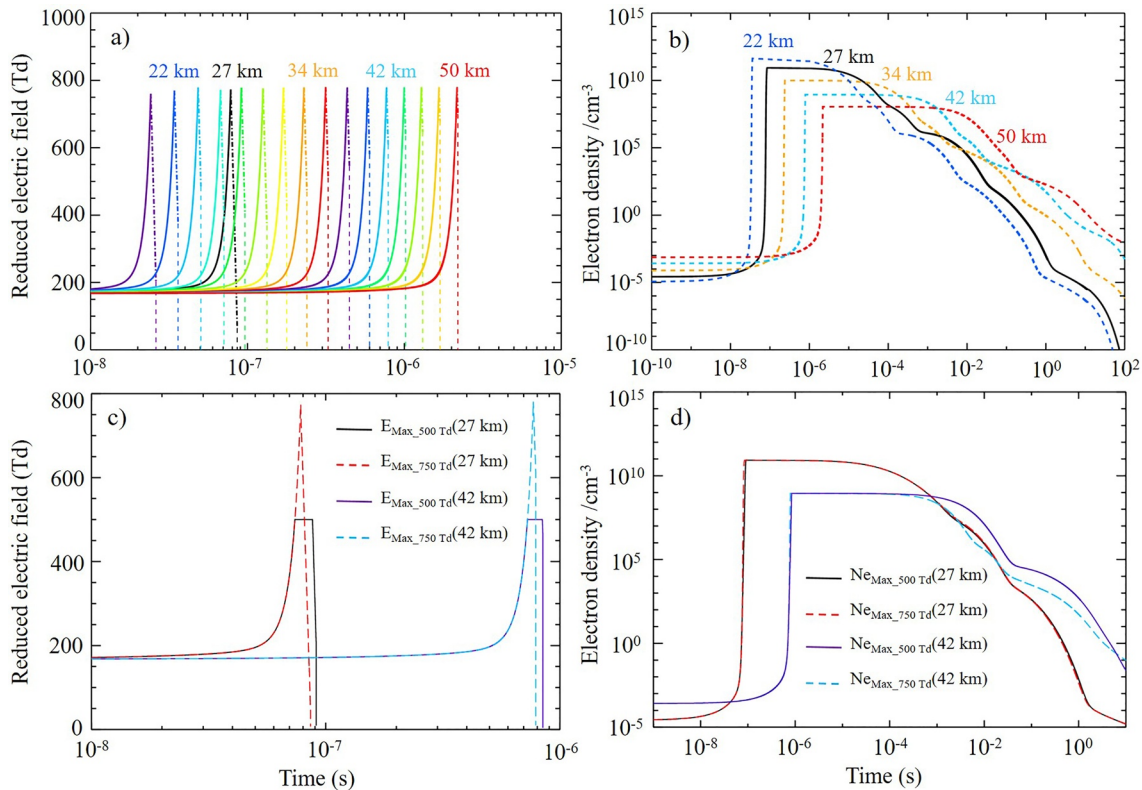


Figure 1. Time evolutions of (a) electrodynamic reduced electrical fields (Td), and (b) simulated electron density (cm^{-3}) at altitudes from 20 to 50 km (every 2 km), alongside the time evolutions of (c) capped reduced electrical fields (Td), and (d) the resulting electron density (cm^{-3}) at altitudes of 27 and 42 km by using the peak electric field values of 500 and 750 Td.

bromine chemical families associated with stratospheric ozone as well as the ions and excited species. A detailed description of the streamer part of the model and its validation exercise at 27 km can be found in Xu et al. (2020). To investigate the chemical processes associated with a single streamer and leader of BJ, the effect of convection is not considered in this model.

2.2. Streamer Parameterization

During the streamer discharge processes, the production and the loss of electrons are driven by ionization and attachment processes, which depend on the local electric field. Instead of using a simple electric field with a constant pulse (e.g., Gordillo-Vázquez, 2008; Sentman et al., 2008; Winkler & Notholt, 2014, 2015), the MiPO-Streamer model uses a realistic streamer electric field time evolution during the discharge process obtained from a self-consistent electrodynamic streamer model (Ihaddadene & Celestin, 2017). This realistic streamer parameterization has been previously developed by Xu et al. (2020) and applied at an altitude of 27 km to represent the streamer discharge, including the rising electric field (kV/m) stage (S_i) and the decreasing field stage (S_{ii}) after it reaches its maximum. Compared to the widely used constant pulse parameterization, Xu et al. (2020) highlighted at 27 km that this realistic electric field of the streamer induces non negligible impact on chemistry compared to simulation with a simple electric field pulse. Thus, this study generalize the realistic electric field of 27 km to the studied altitudes from 20 to 50 km by scaling the electric field fit function and the time through:

$$E_{\text{altitude}}(t) = E_{27 \text{ km}} \left(t \times \frac{N_{\text{altitude}}}{N_{27 \text{ km}}} \right) \times \frac{N_{\text{altitude}}}{N_{27 \text{ km}}}.$$

According to Raizer et al. (2007), the electron density at the end of the electric field ($n_{e,\text{end}}$) is on the order of $10^{14} \left(\frac{N}{N_0} \right)^2 \text{cm}^{-3}$, where N is local air density and N_0 is air density at the Earth's surface. The $n_{e,\text{end}}$ at each altitude is deduced from the $n_{e,\text{end}}$ at 27 km by using the scale factor of $\left(\frac{N_{\text{altitude}}}{N_{27 \text{ km}}} \right)^2$. Then the electron densities decrease from their maximum as a function of altitude (Figure 1b).

Several simulations were performed to adapt both S_i and S_{ii} stages (increase and decrease stages) of the reduced electrical fields. The time evolutions of the reduced electrical fields considered and the simulated electron densities associated from 20 km up to 50 km are presented in Figures 1a and 1b, respectively. Although the streamer electric field parameterization used for different altitudes produces peak values around 750 Td, which exceed the measured value of 500 Td (Hoder et al., 2016), the simulation results obtained using both electric fields exhibit similar outcomes (Figures 1c and 1d), due to the similar saturated electron density achieved at the corresponding altitude. The total electric field durations (both stages) at high altitudes are longer (e.g., 2.2 μ s at 50 km) than those at low altitudes (e.g., 2.4×10^{-2} μ s at 20 km). The time evolutions of electron density at all altitudes present the same shape with abrupt increases and slow decreases during roughly 100 s.

2.3. Leader Representation

The discharge of the leader part occurs after the discharge of the streamer part at one given point, and it propagates from 20 to 28 km assumed in this study (Da Silva & Pasko, 2013). It is characterized by a strong increase in gas temperature, and its reduced electric field is lower than that of the streamer discharge. The electron process is driven by the thermal ionization and the decomposition of nitrogen and oxygen species (Aleksandrov et al., 1997). To represent this discharge of the leader part, we consider the set of high-temperature reactions and their corresponding reaction coefficients as Winkler and Notholt (2015), which was deduced from a kinetic model of Aleksandrov et al. (1997). The leader parameters at studied altitudes, such as leader discharge durations, values of electric field (60 Td) and translational temperature are set the same as Winkler and Notholt (2015).

As shown in Figure 15a of Da Silva and Pasko (2013), the leader discharge begins on the order of 1×10^{-4} s after the streamer part on average, in the studied leader altitude range of 20–30 km with electric currents ranging from 1 to 100 A. The streamer-to-leader transition times of 1×10^{-4} s and 100 s (which was used in Winkler & Notholt, 2015) were evaluated and the results showed that variations in the main chemical concentrations from the two times disappeared within seconds, suggesting that the impact of varying transition times is not significant for chemical estimation, especially over long time-scales (e.g., hours or days). Therefore, the more reasonable transition time of 1×10^{-4} s is used in the simulations, instead of 100 s.

Due to the spatial extent of the leader, it is necessary to consider diffusion in the high-temperature core of the leader. We consider an electrodynamic column radius of the order of 10 m that varies with altitude, as assumed by Winkler and Notholt (2015). Molecular diffusion is applied to the chemical species of O_3 , NO_2 , NO , and N_2O , and their diffusion coefficients at studied altitudes are obtained based on sources such as Chapman and Cowling (1970) and Davis (1983). The gas chemistry and diffusion solved sequentially by using an operator-splitting scheme, with time steps that may vary between the two processes. When the density of chemical species is equal to its background density (the density of no discharge case), the diffusion process stops (equilibrium status) in the core of the leader. For more details about the conducted diffusion process in the model, please refer to Xu and Zhang (2023).

Above all, in comparison to the modeling method used in Winkler and Notholt (2015), the approach employed in this study considers a greater number of chemical species (including chlorine and bromine) and reactions (Winkler & Notholt, 2015 did include chlorine, although they did not discuss its variation), incorporates more reasonable parameters for reaction rates, electrical field, streamer-to-leader transition time, and diffusion processes, and simulates for a longer duration (Xu et al., 2020). These differences result in varying outcomes between the two studies.

2.4. Initialization

This study chooses to investigate in detail an event reported by Chou et al. (2011), which was the first ground-based observed type II gigantic jet over a thunderstorm in the Fujian province, China, on 22 July 2007 from the Lulin Observatory (121°E, 23°N) in Taiwan by three sight-aligned WATEC 100-N cameras. The generation sequence started with a blue starter, followed by a BJ that occurs at the same cloud top after \sim 100 ms. The BJ then developed into a gigantic jet \sim 50 ms later. The simulations in this study start during nighttime at 12:00 UTC and are performed every 2 km from 20 to 50 km.

The initial values of temperature, pressure and all gaseous species mixing ratios come from the three-dimensional chemistry-transport model for ruling the Ozone Budget in the Stratosphere (REPROBUS) Model (Lefèvre

et al., 1994) with daily forecasts on AERIS data center from 0 to 90 km (<http://cde-espri.ipsl.fr/>). To determine the initial electron density at night time, this study used: $N_e = \frac{1.7 \times 10^{13}}{N}$, where N is the local air density, in cm^{-3} (MacGorman & Rust, 1998, p. 34; Mitchell & Hale, 1973). The initial values of all the ion species are set to zero for streamer simulations.

3. Impact of BJ Discharge on Ozone From 20 to 50 km

We investigate the impact of BJ (considering both streamer and leader discharges) on stratospheric ozone VMRs as a function of altitude through the 2-day simulations by the MiPO-Streamer model. Nine time points of interest after the electric breakdown of BJ streamers and leader are selected: 10^{-4} s, 10^{-2} s, 0.2 s, 0.5 s, 0.7 s, 100 s, 12.9 hr, 24 hr, and 48 hr. The first two time points are selected to investigate the streamer discharge chemical impact, 0.2, 0.5, and 0.7 s are selected to follow the leader discharge chemical impact up to 30 km, 100 s indicates the early impact of the BJ discharge and the last three time points are selected to investigate the interactions between the plasma chemistry induced by the BJ discharge and the neutral chemistry associated with O_3 during two diurnal variations. Among them, 12.9 hr corresponds to daytime (zenith angle is 45°), and the other times are in the nighttime.

3.1. Below 30 km: Streamer and Leader Impact

From 20 to 30 km, the stratospheric chemistry is perturbed by both streamer and leader discharges. This part focus on four time points of interest (10^{-4} , 10^{-2} , 0.2 and 0.7 s) for investigating the chemical impact of both streamer and leader discharges considering the diffusion effect. Among them, 0.2 s is around the duration times of leader discharge at these studied altitudes, and 0.7 s is the duration time of high temperature decreasing to the air temperature which is consistent with the 0.5 s after the end of the leader phase between 18 and 27 km considered by Winkler and Notholt (2015).

To investigate the impact both of the streamer and the leader channel, the obtained results presented in Figure 2 are O_3 , O, and NO_x vertical VMRs profiles by considering the plasma chemistry associated with streamer and leader discharge and diffusion processes (BJ-simulation), the plasma chemistry associated with streamer discharge without diffusion (S -simulation), and the only neutral chemistry without discharge (N -simulation) every 2 km from 20 to 30 km at the four time points of interest. As the duration time of leader discharge linearly decreases from about 167 ms at 20 km to zero at 30 km (Winkler & Notholt, 2015), the BJ-simulation presents the same results as those of the S -simulation at 30 km.

Comparing the results of N -simulation and S -simulation, the O_3 VMRs of S -simulation increase strongly at 10^{-4} and 10^{-2} s (Figures 2a and 2b) and this increase is maintained at 0.7 s (Figures 2c and 2d). The streamer discharge produces atomic oxygen by electric-driven reactions, and it rapidly converts to O_3 through:



The impact of the leader discharge from the BJ-simulations (black solid line) can be seen at 10^{-4} and 10^{-2} s with O_3 VMRs increased at altitudes from 20 to 24 km, and slightly decreased above 24 km (Figures 2a and 2b).

The production of O_3 VMRs at low altitudes are due to the conversion of atomic oxygen (as those of S -simulations reaction [Equation 1]) with additional atomic oxygen produced during the leader discharge (as shown in Figures 2e and 2f) through the high-temperature reactions:



The O_3 depletion at high altitudes are due to the small production of atomic oxygen by leader discharge and the large production of NO_x through the streamer and the leader discharges (Figures 2i and 2j). Then the catalytic cycle with NO_x is efficient:



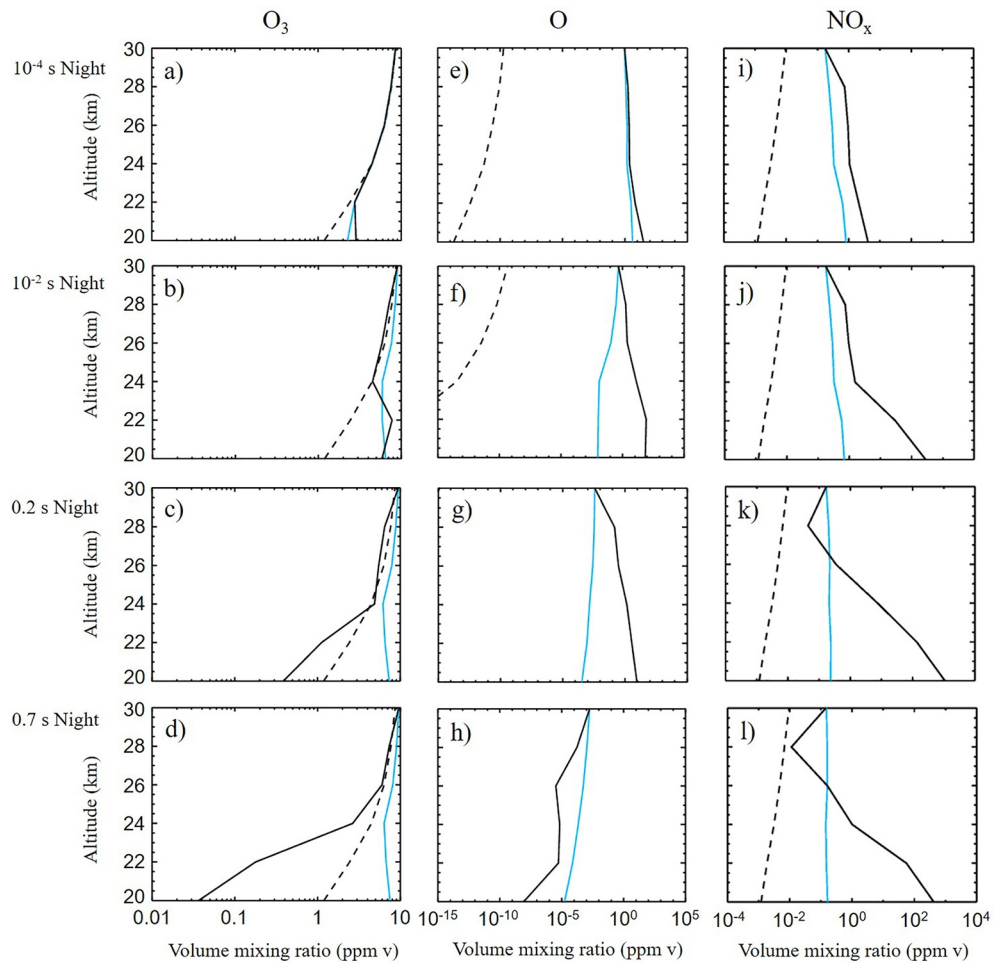


Figure 2. Vertical profiles of O_3 , atomic oxygen (O) and NO_x volume mixing ratios (in column) at selected time points of interest at 10^{-4} , 10^{-2} , 0.2, 0.7 s (in row), on 22 July 2007 at (121°E, 23°N) by the Microphysical Photochemical Ozone Streamer model simulations. Black dotted line: N -simulation (without discharge), blue line: S -simulation (with plasma chemistry associated with streamer discharge), black solid line: blue jet-simulation (with plasma chemistry associated with streamer and leader discharge, and diffusion processes).



At 0.2 s (the end of leader discharge), the O_3 VMRs of BJ-simulation are lower than those of both the N - and S -simulation at most studied altitudes. At altitudes lower than 24 km (Figure 2d), O_3 VMRs of BJ-simulation at 0.7 s decrease to smaller values than those at 0.2 s. Those O_3 depletion are caused also by the NO_x catalytic cycle (reactions [Equations 5–7]) with the largely produced and maintained NO_x of BJ-simulation (Figures 2j–2l) compared to S -simulation. The high-temperature chemistry leads to NO_x increase mainly through the reactions (Equation 3) and:



whereas the O_3 VMRs of BJ-simulation at the altitudes of 26 and 28 km increase are close to those of N -simulation at 0.7 s, the slight depletion exists due to catalytic NO_x cycle and the diffusion effect (Figures 2k and 2l).

Compared to the S -simulation at 0.7 s, BJ-simulation shows less O_3 abundance as reported by Winkler and Notholt (2015), while only by three orders of magnitude at 20 km in our study (N -simulation is at 10^{13} cm^{-3} , and BJ-simulation is at 10^{10} cm^{-3} . Note that the x -axis of Figure 2d is in logarithmic scale) and five orders of

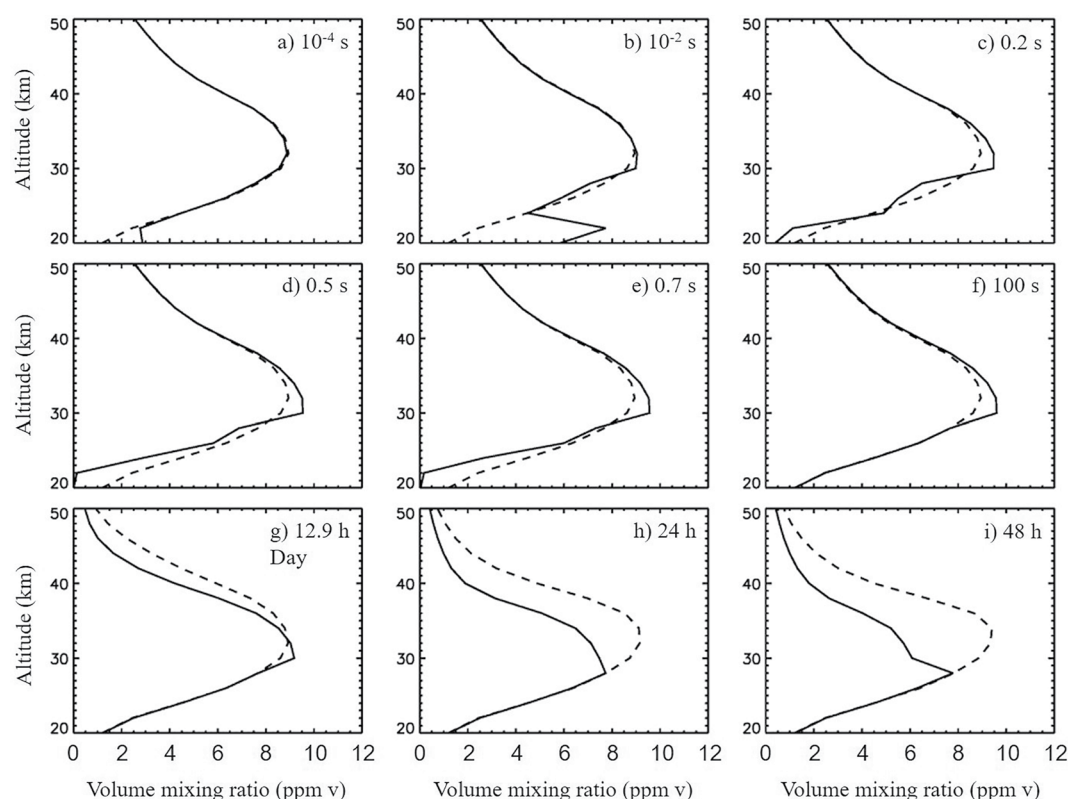


Figure 3. Vertical profiles of O_3 at nine selected time points of interest at 10^{-4} s, 10^{-2} s, 0.2 s, 0.5 s, 0.7 s, 100 s, 12.9 hr, 24 hr, and 48 hr, on the 22 July 2007 at $(121^\circ E, 23^\circ N)$ by the Microphysical Photochemical Ozone Streamer model simulations. Dotted line: N -simulation (without discharge), solid line: blue jet (BJ)-simulation (with plasma chemistry associated with BJ discharge, and the diffusion processes at altitudes from 20 to 28 km).

magnitude in Winkler and Notholt (2015). Tracking the time evolution of chemical species associated with O_3 (e.g., N, O, which are not shown here), their time evolutions and density values are similar to those displayed by Winkler and Notholt (2015). Therefore, this is probably due to different diffusion, and the less increased NO_x density of BJ-simulation (at 20 km is $\sim 8 \times 10^{14} \text{ cm}^{-3}$) than that of Winkler and Notholt (2015) ($\sim 1.8 \times 10^{15} \text{ cm}^{-3}$).

3.2. Results in the 2-Day Simulations

In this part, we will present the chemical impact of BJ discharge in the whole stratosphere (from 20 to 50 km) in the 2-day simulations, including the BJ streamer impact at the altitude range of 30–50 km, and the combined BJ streamer and BJ leader (with diffusion during the first 2 hr and the equilibrium is reached) impact at the altitude range of 20–28 km. Figure 3 shows the O_3 VMR vertical profiles obtained from 20 to 50 km at nine selected time points of interest at (a) 10^{-4} s, (b) 10^{-2} s, (c) 0.2 s, (d) 0.5 s, (e) 0.7 s, (f) 100 s, (g) 12.9 hr, (h) 24 hr, and (i) 48 hr. The dotted line corresponds to the simulation without discharge (N -simulation), and the solid line is the simulation with plasma chemistry associated with BJ discharge.

During the early stage of the BJ discharge (first 100 s), compared to the N -simulation, O_3 VMR drastically increases in the low stratosphere from 20 to 22 km at 10^{-4} and 10^{-2} s (Figures 3a and 3b). These excess produced O_3 are then consumed, with complete destruction at 20 km at 0.2 s, and O_3 VMRs are lower than those obtained in N -simulation at 0.5 and 0.7 s. This ozone loss is due to the high production of NO_x in the low levels due to leader high-temperature chemistry (see previous Figures 2k and 2l) and the catalytic cycle associated. The O_3 depletion is less efficient as altitude increases with roughly 0.5 ppm v at 28 km and 1 ppm v at 20 km at 0.7 s. After 100 s in these low altitude levels (20–28 km), O_3 VMRs recover their initial values which are similar to those of the N -simulation (without the discharge) due to diffusion. At the end of the BJ-simulation, the O_3 VMRs remain the same value as N -simulation. It is possible to conclude that the perturbation of O_3 VMRs only lasts in the first 100 s at low altitudes.

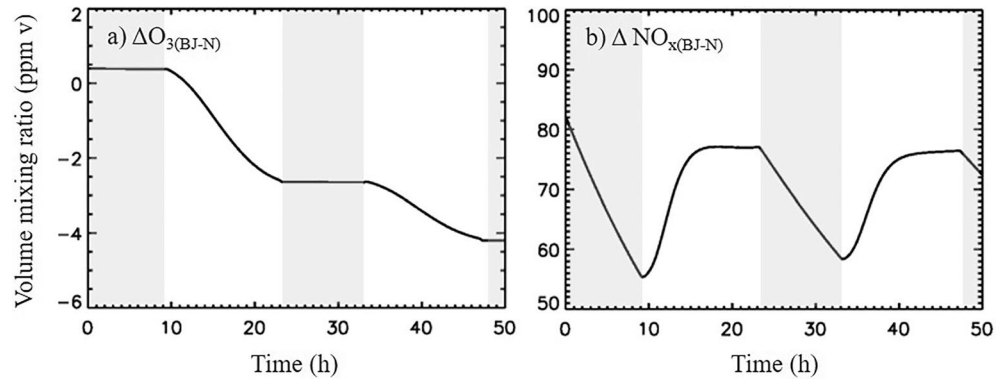


Figure 4. Time evolutions at 34 km of O_3 and NO_x volume mixing ratios differences between the blue jet (BJ)-simulation and the N -simulation. Night-time periods are in gray. $\Delta O_3(BJ-N) = O_3(BJ\text{-simulation}) - O_3(N\text{-simulation})$, $\Delta NO_x(BJ-N) = NO_x(BJ\text{-simulation}) - NO_x(N\text{-simulation})$.

In the middle stratosphere (the altitude range of 30–36 km), the BJ discharge perturbation starts at 10^{-2} s with an enhancement of O_3 VMRs (Figure 3b) and it increases to 10 ppm v (+1 ppm v compared to the N -simulation) at 100 s at the maximum values of the ozone layer. There is no obvious change of the O_3 VMRs in the upper stratosphere (~40 to 50 km) during the first 100 s.

After 100 s, at the daytime of 12.9 hr (Figure 3g), O_3 depletion of BJ-simulation appears at an altitude range of 32–50 km (middle and upper stratosphere) compared to the N -simulation. O_3 VMRs continue to decrease at 24 and 48 hr in the middle stratosphere. For instance, in comparison with N -simulation, the O_3 VMRs decrease 2.5 ppm v and -4.2 ppm v after 24 and 48 hr respectively at 34 km of BJ-simulation. Roughly half of the ozone is destroyed at the maximum VMR of the ozone layer after 48 hr. In this range of altitudes up to 50 km, ozone depletion is mainly supported through the well-known NO_x , ClO_x and BrO_x catalytic cycles (Portmann et al., 2012). After 2 days of BJ-simulation, the maximum of O_3 VMR is significantly reduced at altitudes between 30 km up to 50 km. This reduction is comparable to the findings of Pérez-Invernón et al. (2019), who obtained a O_3 reduction between 24 and 45 km after a 10-year simulation (as depicted in Figure 11 of their study). However, the O_3 density observed in this study is 2–4 times lower than that of Pérez-Invernón et al. (2019). The maximum amount of consumed O_3 is more than -60% compared to the N -simulation, which occurs at 38 km. Whereas, the O_3 reduction shown by Pérez-Invernón et al. (2019) was just around -10% at 30–40 km at this studied latitude (23°N). This difference can be attributed to the larger amount of produced NO_x in this study (500%, Figure 4b) compared to Pérez-Invernón et al. (2019) (~10%, see Figure 8 of their study). This difference can be due to the use of the chemical impact of BJ at 0.5 s from Winkler and Notholt (2015), rather than the impact at a longer time after discharge for the streamer zone when the NO_x continued to increase due to the convective of the active atoms (N and O) produced during the discharge process. Besides, the disparity may be attributed to the shorter simulation period conducted in this study (2 days), as compared to Pérez-Invernón et al. (2019) (in years), which could potentially be impacted by the variations of long-lived chemical species. The ozone layer appears to be weaker and to “shift” in altitude in terms of the vertical location of O_3 VMR maximum from 34 km down to 28 km.

To follow more in detail what happened during the 2 days of simulation, Figure 4 presents the time evolutions at 34 km of the O_3 and NO_x VMRs differences obtained through BJ-simulation minus N -simulation.

At 34 km, just after the BJ discharge, the O_3 VMR difference ($\Delta O_3(BJ-N)$) is marginally enhanced by 0.4 ppm v (the initial O_3 VMR is 8.8 ppm v) and the NO_x difference ($\Delta NO_x(BJ-N)$) attains 82 ppb v (Figures 4a and 4b). BJ discharge produces a very strong amount of NO_x (the initial NO_x VMR is 14 ppb v).

Then the time evolutions of both $\Delta O_3(BJ-N)$ and $\Delta NO_x(BJ-N)$ present diurnal cycles which for $\Delta O_3(BJ-N)$ not neglectable decrease during the daytime and constant values during night-time, and for $\Delta NO_x(BJ-N)$ decrease during night-time, followed by an increase and constant value during daytime. During the second daytime, the decreased $\Delta O_3(BJ-N)$ is 1.6 ppm v, which is smaller than that during the first daytime (3 ppm v). In parallel, the production of NO_x by the BJ discharge at 34 km is little consumed during the first diurnal cycle (initially is +82 ppb v and at 24 hr is +77 ppb v, Figure 4b) and no significant change during the second diurnal cycle (+76 ppb v at 48 hr).

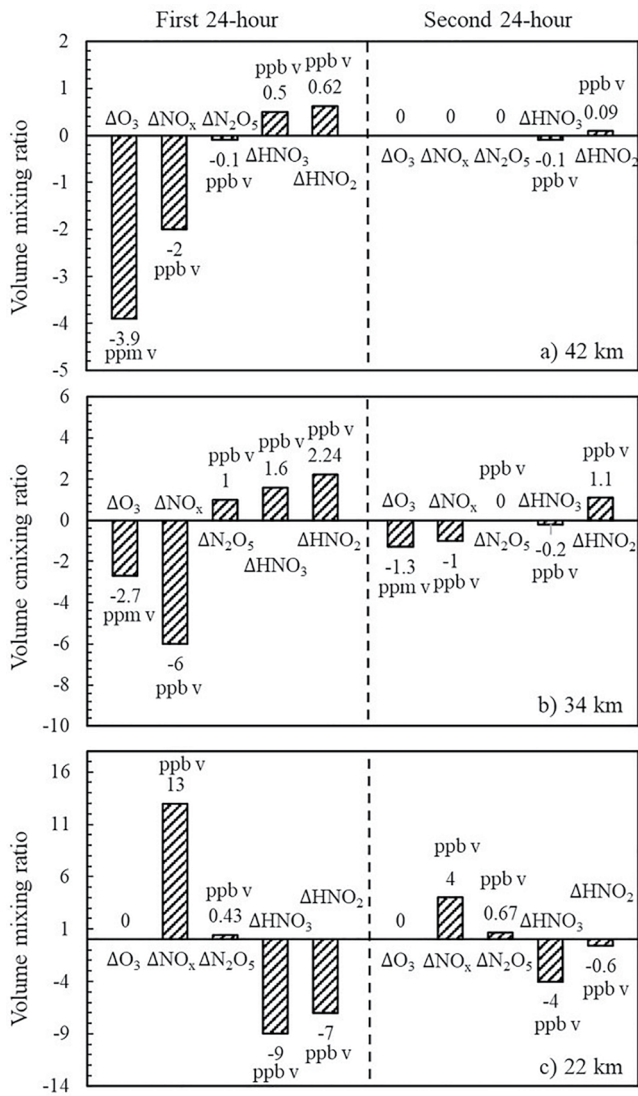


Figure 5. Changes in the volume mixing ratios of O_3 , NO_x , N_2O_5 , HNO_3 , and HNO_2 during the first 24 hr (e.g., $\Delta NO_x\text{-first} = NO_x [24 \text{ hr}] - NO_x [100 \text{ s}]$) and second 24 hr (e.g., $\Delta NO_x\text{-second} = NO_x [48 \text{ hr}] - NO_x [24 \text{ hr}]$) of blue jet simulation at (a) 42 km, (b) 34 km, (c) 22 km.

Most of the NO_x VMRs produced by the BJ are maintained during the 2-day simulation and a new equilibrium seems to appear in the NO_y family.

The obvious O_3 depletion by BJ discharge at 34 km is caused by the NO_x catalytic cycle, as the NO_x produced by BJ discharge is maintained. Due to neutral chemistry, the O_3 VMR decreases critically during the 2-day simulation at 34 km with more than 40% of ozone consumed by the excess of NO_x produced by the discharge.

4. Discussion

While the NO_x produced by the BJ discharge continued to affect O_3 abundance during the 2 days of simulation, it is interesting to look at the perturbations in the partitioning of the neutral species included in the nitrogen family (NO_y) and the chlorine and bromine family (Cl_y , Br_y). To do that, we select three altitudes of 42, 34, and 22 km to analyze the budget (production and loss) of the investigated chemical family. In this section, L(species) and P(species) stand for the loss and production of studied chemical species, respectively.

4.1. NO_y Family Budget During the Two Diurnal Cycles

To understand the impact of the BJ discharge on neutral chemistry, the major VMRs changes in the NO_y family during the two diurnal cycles of the BJ-simulation are investigated in this part. The major changes are associated with NO_x , N_2O_5 , HNO_3 , and HNO_2 VMRs. Figure 5 presents these VMRs changes during each diurnal cycle (e.g., $\Delta NO_x\text{-1st} = NO_x [24 \text{ hr}] - NO_x [100 \text{ s}]$ and $\Delta NO_x\text{-2nd} = NO_x [48 \text{ hr}] - NO_x [24 \text{ hr}]$, with the same calculation for other species) and those of ozone at 42, 34, and 22 km. The chemical species N_2O_5 and HNO_3 have longer lifetimes than NO and NO_2 in the stratosphere.

At 42 km, the impact of the BJ and neutral chemistry induced O_3 loss ($L[O_3] = -3.9 \text{ ppm v}$) only during the first diurnal cycle. NO_x and N_2O_5 VMRs are lost ($L[NO_x] = -2 \text{ ppb v}$ and $L[N_2O_5] = -0.1 \text{ ppb v}$), and HNO_3 and HNO_2 VMRs are produced ($P[HNO_3] = +0.5 \text{ ppb v}$ and $P[HNO_2] = +0.62 \text{ ppb v}$) (Figure 5a). Regarding the budget at this altitude, the absolute value $L[NO_x] + 2 \times L[N_2O_5]$ is slightly greater than $P[HNO_3] + P[HNO_2]$, it means that the NO_x produced by the BJ discharge probably contributes to other reservoirs. Note that the MiPO-Streamer model due to its semi-implicit symmetric resolution scheme keeps exactly constant the number of atoms (Ramaroson et al., 1992). During the second diurnal cycle at this altitude, the production/loss of NO_x , N_2O_5 , HNO_3 , and HNO_2 are very small and O_3 is not affected. These analyses indicate that a new “equilibrium” is reached in the neutral chemistry after 24 hr, with most of the NO_x VMR early produced by the BJ discharge maintained and a strong enhancement of HNO_3 and HNO_2 multiplied by more than 4 (compared to the N -simulation during the first diurnal cycle with the VMR of $+0.2 \text{ ppb v}$ for HNO_3 , and $+0.15 \text{ ppb v}$ for HNO_2).

At 34 km, O_3 loss is 2.7 ppb v during the first diurnal cycle and $L[NO_x] = -6 \text{ ppb v}$, $P[N_2O_5] = +1 \text{ ppb v}$, $P[HNO_3] = +1.6 \text{ ppb v}$, $P[HNO_2] = 2.24 \text{ ppb v}$ (Figure 5b). As $L[NO_x] \approx 2 \times P[N_2O_5] + P[HNO_3] + P[HNO_2]$, most of the consumed NO_x are converted into N_2O_5 , HNO_3 , and HNO_2 through the following reactions:



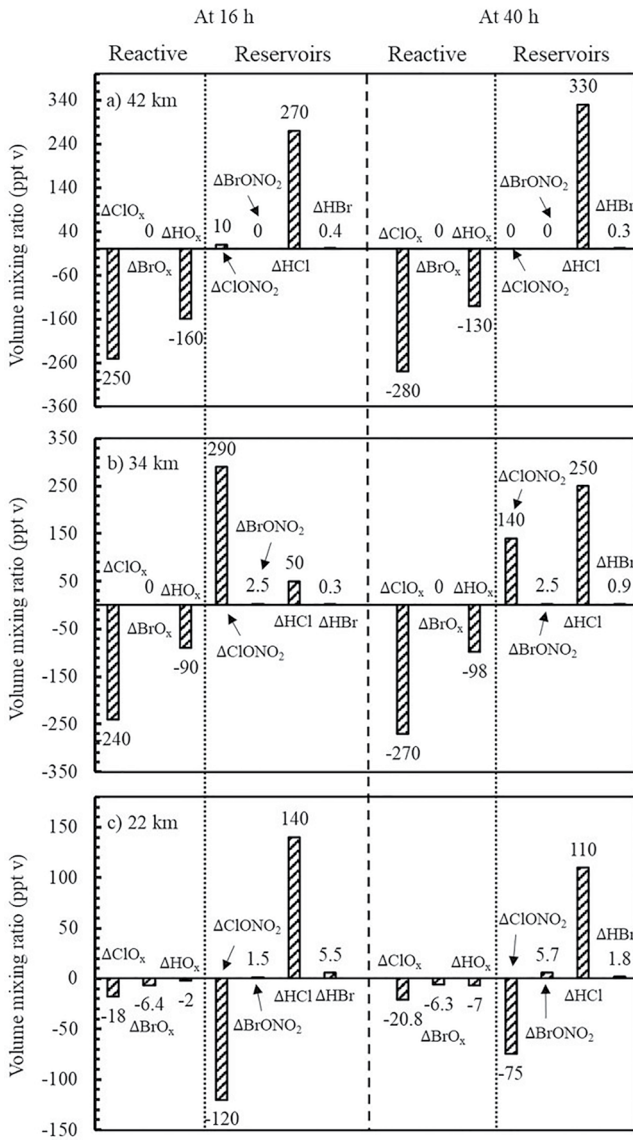
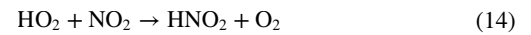


Figure 6. The ClO_x , BrO_x , HO_x , ClONO_2 , BrONO_2 , HCl , and HBr volume mixing ratios differences between the discharge and the no-discharge simulations (e.g., $\Delta\text{ClO}_x = \text{ClO}_x(\text{BJ-simulation}) - \text{ClO}_x(\text{N-simulation})$), and the same for other presented species) at 16 and 40 hr (corresponding to 12:00 LT) for altitudes of 42, 34, and 22 km.

Figure 6a shows the obvious reduction of ClO_x and HO_x VMRs ($L[\text{ClO}_x] = -250$ ppt v; $vL[\text{HO}_x] = -160$ ppt v) and the enhancement of HCl VMR ($P[\text{HCl}] = +270$ ppt v) in the BJ-simulation at 42 km which highlights that ClO_x and HO_x mainly contribute to HCl production by:



Moreover, the O_3 depletion rates due to ClO_x and HO_x at 42 km are efficient (Portmann et al., 2012), their small VMRs in the BJ-simulation reduce the contributions for the O_3 depletion at this altitude. The conversion of ClO_x and HO_x reactive species into HCl reservoir species persists during the second day with +330 ppt v. As a consequence, the equilibrium in the partitioning of the Cl_y family is not attained at 48 hr and the major reservoir impacted by the BJ perturbation is HCl (an increase of 8.5%).



The NO_x produced by the BJ discharge are mainly converted to N_2O_5 , HNO_3 and HNO_2 at 34 km. The impact of the BJ discharge on ozone and partitioning of the NO_y family continues during the second diurnal cycle.

During the first 24-hr period at 22 km (Figure 5c), the results are very different from those at 34 and 42 km. No O_3 changes occurred after 100 s, as the direct production of ozone by the BJ discharge (streamer followed by leader stage) has been consumed and homogenized with the environment due to the diffusion processes in the first 100 s (Figure 3). Concerning the changes of the NO_y family during the first diurnal cycle, there is production of NO_x and N_2O_5 ($P[\text{NO}_x] = +13$ ppb v; $P[\text{N}_2\text{O}_5] = +0.43$ ppb v) and loss of HNO_3 and HNO_2 ($L[\text{HNO}_3] = -9$ ppb v; $L[\text{HNO}_2] = -7$ ppb v). The same behavior occurs, but in a lesser way, during the second diurnal cycle. It means that the equilibrium of the NO_y family is not attained after 48 hr of the simulation, and the increase of NO_x reactive species and the decrease of nitric acid impacted by the BJ discharge lasts more than 2 days.

Above all, as a function of altitude, neutral chemistry does not answer the stress of the discharge in the same way. At 42 km, the perturbation in the NO_y family leads to a rapid new equilibrium after 24 hr. At 34 km, the equilibrium in the NO_y family is not complete after 24 hr, and NO_x species VMRs continue to decrease slightly during the second diurnal cycle. In the low stratosphere, at 22 km, NO_x species VMRs increase during the 2 days of simulation in parallel with the HNO_3 and HNO_2 VMR decrease, and the equilibrium is not attained after 48 hr.

Moreover, whatever the altitude is, the additional species in the family of Cl_y and Br_y must be studied as they are in direct relationship with NO_x and NO_y budget (like ClONO_2 and BrONO_2) and impact ozone via catalytic cycles.

4.2. BJ Discharge Impact on Neutral Chemistry: HO_x and Cl_y , Br_y Families

Figure 6 displays the differences in reactive chlorine ClO_x , bromine BrO_x and hydrogen HO_x , and reservoir ClONO_2 , BrONO_2 , HCl and HBr VMRs between the BJ-simulation and the N-simulation (e.g., $\Delta\text{ClO}_x = \text{ClO}_x(\text{BJ-simulation}) - \text{ClO}_x(\text{N-simulation})$) and the same for other presented species) at 42, 34, and 22 km. As the reactive species ClO_x , BrO_x , and HO_x are abundant in the daytime, the differences at 16 and 40 hr (local time is 12:00) have been selected. Because the bromine family has similar chemical processes as the chlorine family but is less abundant in the stratosphere, therefore, only the chlorine family will be discussed in the following.

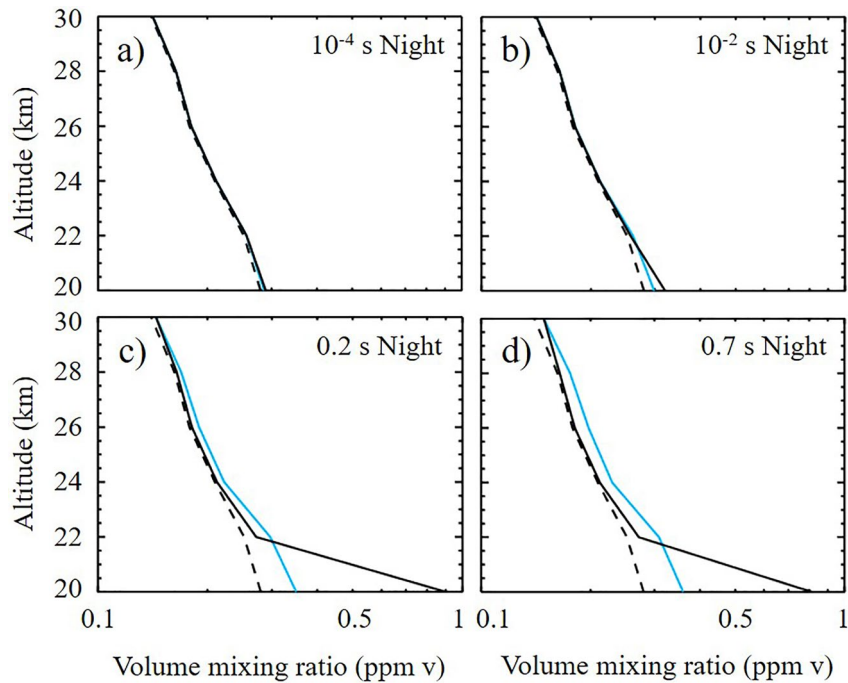


Figure 7. As in Figure 2, but for N_2O .

At 34 km, Chlorine reservoirs of both $ClONO_2$ and HCl VMRs are enhanced during the 2 days, coming from ClO_x and HO_x VMRs loss (Figure 6b) through the reaction (Equation 15) and reaction:



The enhancements of $ClONO_2$, HCl , and $BrONO_2$ due to the BJ discharge in the middle and upper stratosphere are not neglectable (with an increase of 88 (44)%, 1.4 (11.8)%, 625 (400)% for $ClONO_2$, HCl and $BrONO_2$ at 16 (40) hr, respectively), because these reservoir species have long lifetimes (HCl roughly 2 years) in the stratosphere. They can be transported over long distances and be reactivated later to destroy ozone.

Different from the two higher altitudes, at 22 km, the $ClONO_2$ reservoir is reduced by the impact of the BJ discharge (Figure 6c) when the reactive species of ClO_x and HO_x are reduced, while HCl VMR is largely enhanced. The $ClONO_2$ is converted into ClO_x due to the atomic oxygen production associated with the BJ discharge:



Then the produced ClO VMR is converted into HCl VMR by reaction (Equation 15). The abundant production of HCl and the $ClONO_2$ loss persist during the second daytime.

Whatever the altitude considered, the perturbation in Cl_y and Br_y family persists after 40 hr of simulation, which means that the equilibrium is not attained after 2 days. The BJ discharge impacts the perturbation of Cl_y and Br_y family more than 40 hr after the event by enhancement of reservoirs ($ClONO_2$, HCl , $BrNO_2$, and HBr) in different ways as a function of altitude. At the maximum of ozone VMR, this increase is about 11.8% for HCl and 44% for $ClONO_2$ after 40 hr of simulation. This is important because of the long lifetime of these species, which could be reactivated later after transport and destroy ozone.

4.3. N_2O Change Variation Impacted by BJ

As shown in Figure 7, N_2O VMRs slightly increased from 20 to 24 km at 10^{-4} and 10^{-2} s (Figures 7a and 7b). In S -simulations, N_2O is mainly produced through the detachment reaction:



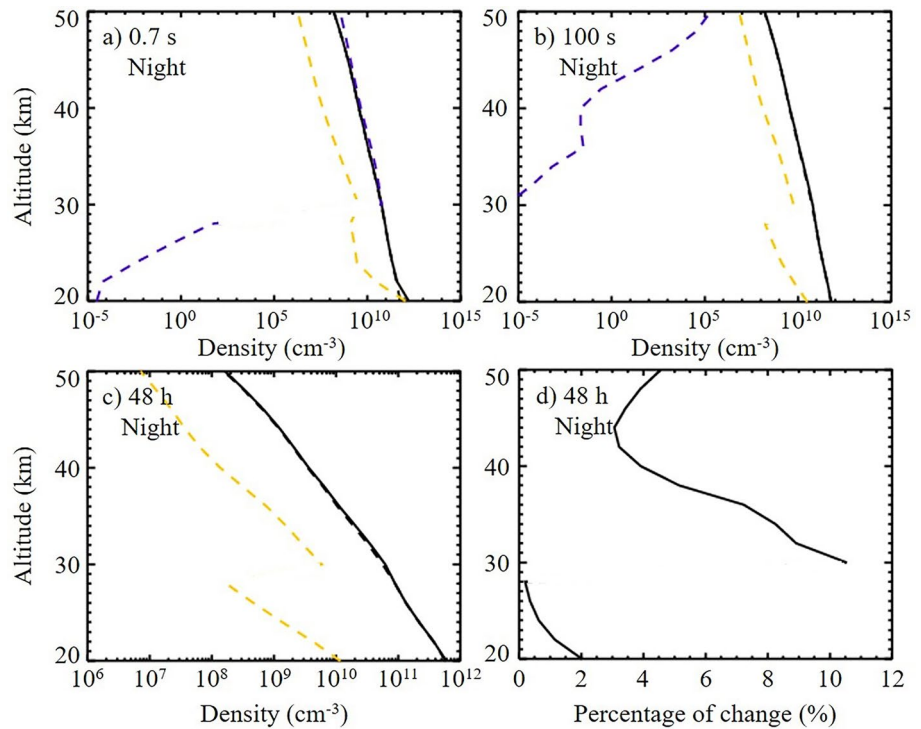


Figure 8. Vertical profiles of N₂O (black, yellow) and N (purple) at (a) 0.7 s, (b) 100 s, and (c) 48 hr, on the 22 July 2007 at (121°E, 23°N) by the Microphysical Photochemical Ozone Streamer model simulations. In (a)–(c), the black dotted line is *N*-simulation (without discharge, which is overlapped with the black solid line), the solid line is blue jet (BJ)-simulation (with plasma chemistry associated with BJ discharge, and the diffusion processes at altitudes from 20 to 28 km), the yellow and purple dotted lines are the difference of N₂O and N density between BJ-simulation and *N*-simulation, respectively. (d) Is the percentage variation of N₂O between BJ-simulation and *N*-simulation after 48 hr.

during the streamer discharge processes, and through the neutral chemistry:



BJ-simulations, on the other hand, produce more N₂O VMRs than *S*-simulations additionally by reaction (Equation 4) during the leader high-temperature process. The consumed N₂O VMRs of leader at 0.7 s (Figure 7d) are due to the diffusion, whereas the *S*-simulations do not take diffusion into account.

Compared to the findings of Winkler and Notholt (2015) (as depicted in Figure 19 of their study, up to 28 km), the produced N₂O density at 0.7 s at 20–28 km is 3–4 orders of magnitude smaller than that reported by Winkler and Notholt (2015). For instance, at 20 km, the N₂O density increased by 10¹² cm⁻³ in this study and by 10¹⁶ cm⁻³ in the Winkler and Notholt (2015). Tracking the time evolution of chemical species associated with N₂O (e.g., N, O, N(²D), N₂(A), which are not shown here), their time evolutions and density values are similar to those displayed by Winkler and Notholt (2015). Therefore, the less produced N₂O density at 20–28 km in this study is mainly caused by the diffusion processes.

After 48 hr simulation, the vertical profile of N₂O density (presented by the black solid line in Figure 8c) is found to be in the same magnitude range as the global average profile of N₂O obtained by Aura-MLS and that obtained from a 10-year simulation with BJ (see Figure 12 of Pérez-Invernón et al. (2019)). Compared to the *N*-simulation, the enhancement of N₂O density in the BJ-simulation (presented by the yellow dotted line in Figure 8c) at the altitude of 30–36 km falls within the range of 10⁸–10¹⁰ cm⁻³, which is similar to that found in the leader channel. Whereas, Pérez-Invernón et al. (2019) noted that the N₂O production by BJ is mainly dominated by the leader phase. It is evident that the produced N is abundant in the streamer zone at 0.7 s (Figure 8a), and continues converting to N₂O through reaction (Equation 19) (Figure 8b). However, Pérez-Invernón et al. (2019) relied on the chemical impact of BJ at 0.5 s from Winkler and Notholt (2015). Moreover, Pérez-Invernón et al. (2019) introduced the chemical impact of BJ as an injection of molecules over a cylindrical area ($R_1 = 2.5$ m and $R_2 = 12.5$ m) from the density increases by Winkler and Notholt (2015), and their results show a high variability depending on the radius.

Furthermore, Figure 8d indicates significant percentage enhancements in N_2O production in the BJ-simulation compared to the N -simulation, particularly in the streamer zone (30–50 km) where the produced N_2O decreases from 10% (at 30 km) to 4.5% (at 50 km). These results agree with those presented by Pérez-Invernón et al. (2019) (refer to Figure 8 in their study), who reported that the BJ produced N_2O decreases from 10% to 3.5% as altitude increases from 30 to 50 km. The leader phase results in a decrease in N_2O production by the BJ from 2% (at 20 km) to $\sim 0.25\%$ (at 28 km), which differs from the findings of Pérez-Invernón et al. (2019) where the percentages decrease from 10% at 20 km to 9.5% at 28 km.

5. Summary and Conclusions

Detailed investigations in the whole stratosphere of the BJ discharge impact on the chemical stratospheric system have been performed during 2 days of simulation with a generalization of the parameterization of the realistic streamer from 20 km up to 50 km. In this study, we consider the effect of BJ streamer discharge in the middle and high stratosphere (30–50 km) and the effect of BJ streamer-leader discharge and diffusion in the low stratosphere (20–28 km). The model used is for a single streamer and leader in this study.

During the first 100 s of simulation, no impact of the BJ discharge occurs on ozone abundance in the upper stratosphere above 40 km, while O_3 is produced in the middle stratosphere associated with the increased atomic oxygen VMRs due to the BJ streamer discharge. In the low stratosphere, O_3 is only produced in the few first 10^{-2} s, and this O_3 excess is drastically consumed through a catalytic cycle associated with a large amount of NO_x produced during BJ leader discharge stage, and the O_3 content is homogenized due to the diffusion processes in the end. After 100 s of simulation, the initial O_3 values are recovered below 28 km.

After the early strong perturbation due to the plasma chemistry (the production of atomic oxygen and NO), the neutral chemistry takes over and impacts the partitioning of the reactive species and reservoirs in the NO_y , Cl_y , and Br_y families for 2 days.

The investigations of BJ discharge simulations during 2 days at different altitudes reveal that the O_3 depletion in the middle and upper stratosphere are mainly due to the NO_x chemical species produced by the discharge through the catalytic cycle. It appears during the two diurnal cycles following the discharge. Because the NO_x VMRs produced by the BJ discharge are efficient for O_3 depletion in the middle stratosphere, the O_3 layer after 2 days of simulation is reduced ($\sim 40\%$ at the O_3 VMR maximum altitude) and appears to “shift” to lower levels (roughly by 6 km). In the low stratosphere, the main reactive chemical changes with NO_x are the conversion between NO_x and their reservoir species (e.g., N_2O_5 , HNO_2 , HNO_3), thus the NO_x produced by the discharge has little impact on O_3 . Meanwhile, the greenhouse gas N_2O shows a significant change throughout the chemical evolution and altitude ranges at 48 hr. The percentage variations of N_2O decreases from 2% (at 20 km) to $\sim 0.25\%$ (at 28 km) in the leader region, and from $\sim 10\%$ (at 30 km) to $\sim 4\%$ (at 50 km) in the streamer zone.

Whatever the altitude considered, the perturbations occur also on the reactive species ClO_x/BrO_x and HO_x , which lead to ozone loss and enhancement of chlorine and bromine reservoirs. The results highlighted that the reactive species of different families have already converted into reservoirs during the two diurnal cycles, meaning that the equilibrium of the neutral chemical system is not attained. In addition, with their long lifetimes in the stratosphere, these reservoir species can be transported over long distances and be reactivated later to destroy ozone.

This study on the detailed chemical impact processes of BJ discharge will help to precisely parameterize BJ discharge effect on stratospheric chemistry, and to improve the studies on the chemical impacts of BJ at a global scale. Here we just consider one streamer and a leader, to achieve that, it is necessary to parameterize the BJ in a two-dimensional model by considering the length of leader channel and the number of streamer branches, including both vertical and horizontal convection. Additionally, to evaluate the total column perturbation of O_3 , NO_x , N_2O and other relevant impacted chemical species over a thunderstorm, and to validate the simulation results by comparing them with measured data in the future study.

Data Availability Statement

The reaction coefficient rates used in this study can be found from the following links: from Winkler and Notholt (2014) (<https://acp.copernicus.org/articles/14/3545/2014/acp-14-3545-2014-supplement.pdf>), and from Jet Propulsion Laboratory (JPL, Sander et al., 2006, <http://hdl.handle.net/2014/41648>). The BOLSIG+ solver, which was used to calculate the reaction rate coefficients of electric field driven processes in this study, is available

for download on the website (Hagelaar & Pitchford, 2005, www.bolsig.laplace.univ-tlse.fr). The output data from the MiPO-Streamer model of this study (including the *N*-simulation, BJ-simulation and *S*-simulation) could be found in <https://drive.google.com/file/d/1hjwGM7ueN5eKNgUCM6uNYQUFv7JdvRB4/view?usp=sharing>.

Acknowledgments

This study was supported by the National Natural Science Foundation of China (No. 42005093), China Postdoctoral Science Foundation (No. E091021801), the Second Tibetan Plateau Scientific Expedition and Research (No. 2019QZKK0104, No. 2019QZKK0604), and the French Research Ministry, the TARANIS project from the Centre National d'Etudes Spatiales (CNES), the Centre National de la Recherche Scientifique (CNRS-INSU), the University of Orleans (UO) and the University Clermont Auvergne (UCA), and the National Key Scientific and Technological Infrastructure project "Earth System Numerical Simulation Facility" (EarthLab). We particularly thank F. Lefèvre for providing us with the chemical data from the REPROBUS CTM model (Lefèvre et al., 1994, <http://cds-espri.ipsl.fr/>). We thank the anonymous reviewers for their time and their detailed and constructive comments that helped to improve the presentation of our results.

References

- Aleksandrov, N. L., Bazelyan, E. M., Kochetov, I. V., & Dyatko, N. A. (1997). The ionization kinetics and electric field in the leader channel in long air gaps. *Journal of Physics D: Applied Physics*, 30(11), 1616–1624. <https://doi.org/10.1088/0022-3727/30/11/011>
- Brognez, C., Huret, N., Eckermann, S., Rivière, E. D., Pirre, M., Herman, M., et al. (2003). Polar stratospheric cloud microphysical properties measured by the microRADIBAL instrument on 25 January 2000 above Esrange and modeling interpretation. *Journal of Geophysical Research: Atmospheres*, 108, 8332. <https://doi.org/10.1029/2001JD001017>
- Chapman, S., & Cowling, T. G. (1970). *The mathematical theory of nonuniform gases*. Cambridge University Press.
- Chou, J. K., Tsai, L. Y., Kuo, C. L., Lee, Y. J., Chen, C. M., Chen, A. B., et al. (2011). Optical emissions and behaviors of the blue starters, blue jets, and gigantic jets observed in the Taiwan transient luminous event ground campaign. *Journal of Geophysical Research: Space Physics*, 116, A07301. <https://doi.org/10.1029/2010JA016162>
- Chuang, C. W., & Chen, A. B. C. (2022). Global distribution and spectral features of intense lightning by the ISUAL experiment. *Journal of Geophysical Research: Atmospheres*, 127(12), e2022JD036473. <https://doi.org/10.1029/2022JD036473>
- Croizé, L., Payan, S., Bureau, J., Duruisseau, F., Thiéblemont, R., & Huret, N. (2015). Effect of blue jets on atmospheric composition: Feasibility of measurement from a stratospheric balloon. *IEEE Journal of Selected Topics in Applied Earth Observations and Remote Sensing*, 8(6), 3183–3192. <https://doi.org/10.1109/JSTARS.2014.2381556>
- Da Silva, C. L., & Pasko, V. P. (2013). Dynamics of streamer-to-leader transition at reduced air densities and its implications for propagation of lightning leaders and gigantic jets. *Journal of Geophysical Research: Atmospheres*, 118(24), 13–561. <https://doi.org/10.1002/2013jd020618>
- Davis, E. J. (1983). Transport phenomena with single aerosol particles. *Aerosol Science and Technology*, 2(2), 121–144. <https://doi.org/10.1080/02786828308958618>
- Goldenbaum, G. C., & Dickerson, R. R. (1993). Nitric oxide production by lightning discharges. *Journal of Geophysical Research: Atmospheres*, 98(D10), 18333–18338. <https://doi.org/10.1029/93jd01018>
- Gordillo-Vázquez, F. J. (2008). Air plasma kinetics under the influence of sprites. *Journal of Physics D: Applied Physics*, 41(23), 234016. <https://doi.org/10.1088/0022-3727/41/23/234016>
- Gordillo-Vázquez, F. J., & Pérez-Invernón, F. J. (2021). A review of the impact of transient luminous events on the atmospheric chemistry: Past, present, and future. *Atmospheric Research*, 252, 105432. <https://doi.org/10.1016/j.atmosres.2020.105432>
- Grossel, A., Huret, N., Catoire, V., Berthet, G., Renard, J. B., Robert, C., & Gaubicher, B. (2010). In situ balloon-borne measurements of HNO₃ and HCl stratospheric vertical profiles influenced by polar stratospheric cloud formation during the 2005–2006 Arctic winter. *Journal of Geophysical Research: Atmospheres*, 115, D21303. <https://doi.org/10.1029/2009JD012947>
- Hagelaar, G. J. M., & Pitchford, L. C. (2005). Solving the Boltzmann equation to obtain electron transport coefficients and rate coefficients for fluid models [Software]. *Plasma Sources Science and Technology*, 14(4), 722–733. <https://doi.org/10.1088/0963-0252/14/4/011>
- Haigh, J. D. (1994). The role of stratospheric ozone in modulating the solar radiative forcing of climate. *Nature*, 370(6490), 544–546. <https://doi.org/10.1038/370544a0>
- Hoder, T., Šimek, M., Bonaventura, Z., Prukner, V., & Gordillo-Vázquez, F. J. (2016). Radially and temporally resolved electric field of positive streamers in air and modelling of the induced plasma chemistry. *Plasma Sources Science and Technology*, 25(4), 045021. <https://doi.org/10.1088/0963-0252/25/4/045021>
- Huret, N., Pommereau, J. P., Dudok de Witt, T., & Pirre, M. (2003). Modeling study of NO_x species in the lower tropical stratosphere over Brazil on February 2001. In *EGS-AGU-EUG Joint Assembly*.
- Ihaddadene, M. A., & Celestin, S. (2017). Determination of sprite streamers altitude based on N₂ spectroscopic analysis. *Journal of Geophysical Research: Space Physics*, 122(1), 1000–1014. <https://doi.org/10.1002/2016JA023111>
- Lefèvre, F., Brasseur, G. P., Folkins, I., Smith, A. K., & Simon, P. (1994). Chemistry of the 1991–1992 stratospheric winter: Three-dimensional model simulations [Software]. *Journal of Geophysical Research*, 99(D4), 8183–8195. <https://doi.org/10.1029/93JD03476>
- Li, D., Luque, A., Gordillo-Vázquez, F. J., Pérez-Invernón, F. J., Husbjerg, L. S., Neubert, T., et al. (2023). Different types of corona discharges associated with high-altitude positive narrow bipolar events nearby cloud top. *Journal of Geophysical Research: Atmospheres*, 128(4), e2022JD037883. <https://doi.org/10.1029/2022JD037883>
- MacGorman, D. R., & Rust, W. D. (1998). *The electrical nature of storms*. Oxford University Press on Demand.
- Mishin, E. V. (1997). Ozone layer perturbation by a single blue jet. *Geophysical Research Letters*, 24(15), 1919–1922. <https://doi.org/10.1029/97GL01890>
- Mitchell, J. D., & Hale, L. C. (1973). Observations of the lowest ionosphere. *Space Research*, 13, 471–476.
- Pérez-Invernón, F. J., Gordillo-Vázquez, F. J., Smith, A. K., Arnone, E., & Winkler, H. (2019). Global occurrence and chemical impact of stratospheric Blue Jets modeled with WACCM4. *Journal of Geophysical Research: Atmospheres*, 124(5), 2841–2864. <https://doi.org/10.1029/2018jd029593>
- Portmann, R. W., Daniel, J. S., & Ravishankara, A. R. (2012). Stratospheric ozone depletion due to nitrous oxide: Influences of other gases. *Philosophical Transactions of the Royal Society B. Biological Sciences*, 367(1593), 1256–1264. <https://doi.org/10.1098/rstb.2011.0377>
- Raizer, Y. P., Milikh, G. M., & Shneider, M. N. (2007). Leader-streamers nature of blue jets. *Journal of Atmospheric and Solar-Terrestrial Physics*, 69(8), 925–938. <https://doi.org/10.1016/j.jastp.2007.02.007>
- Raizer, Y. P., Milikh, G. M., & Shneider, M. N. (2010). Streamer- and leader-like processes in the upper atmosphere: Models of red sprites and blue jets. *Journal of Geophysical Research: Space Physics*, 115, A00E42. <https://doi.org/10.1029/2009ja014645>
- Ramaroson, R., Pirre, M., & Cariolle, D. (1992). A box model for on-line computations of diurnal variations in a 1-D model—Potential for application in multidimensional cases. *Annales Geophysicae*, 10, 416–428.
- Rivière, E. D., Huret, N., Taupin, F. G., Renard, J. B., Pirre, M., Eckermann, S. D., et al. (2000). Role of lee waves in the formation of solid polar stratospheric clouds: Case studies from February 1997. *Journal of Geophysical Research: Atmospheres*, 105(D5), 6845–6853. <https://doi.org/10.1029/1999JD900908>
- Rivière, E. D., Pirre, M., Berthet, G., Renard, J. B., Taupin, F. G., Huret, N., et al. (2002). On the interaction between nitrogen and halogen species in the Arctic polar vortex during THESEO and THESEO 2000. *Journal of Geophysical Research: Atmospheres*, 107(D5), SOL 54–1–SOL 54–11. <https://doi.org/10.1029/2002JD002087>

- Sander, S. P., Golden, D. M., Kurylo, M. J., Moortgat, G. K., Wine, P. H., Ravishankara, A. R., et al. (2006). Chemical kinetics and photochemical data for use in atmospheric studies evaluation number 15 [Dataset]. Jet Propulsion Laboratory, National Aeronautics and Space Administration. Retrieved from <http://hdl.handle.net/2014/41648>
- Sentman, D. D., Stenbaek-Nielsen, H. C., McHarg, M. G., & Morrill, J. S. (2008). Plasma chemistry of sprite streamers. *Journal of Geophysical Research: Atmospheres*, *113*(D11). <https://doi.org/10.1029/2007JD008941>
- Smirnova, N. V., Lyakhov, A. N., & Kozlov, S. I. (2003). Lower stratosphere response to electric field pulse. *International Journal of Geomagnetism and Aeronomy*, *3*(3), 281–287.
- Tomicic, M., Chanrion, O., Farges, T., Mlynarczyk, J., Kolmašova, I., Soula, S., et al. (2023). Observations of elves and radio wave perturbations by intense lightning. *Journal of Geophysical Research: Atmospheres*, *128*(10), e2022JD036541. <https://doi.org/10.1029/2022JD036541>
- Winkler, H., & Notholt, J. (2014). The chemistry of daytime sprite streamers—a model study [Dataset]. *Atmospheric Chemistry and Physics*, *14*(7), 3545–3556. <https://doi.org/10.5194/acp-14-3545-2014>
- Winkler, H., & Notholt, J. (2015). A model study of the plasma chemistry of stratospheric Blue Jets. *Journal of Atmospheric and Solar-Terrestrial Physics*, *122*, 75–85. <https://doi.org/10.1016/j.jastp.2014.10.015>
- Xu, C., Huret, N., Garnung, M., & Celestin, S. (2020). A new detailed plasma-chemistry model for the potential impact of blue jet streamers on atmospheric chemistry. *Journal of Geophysical Research: Atmospheres*, *125*(6), e2019JD031789. <https://doi.org/10.1029/2019JD031789>
- Xu, C., Qie, X., Sun, Z., Yang, J., Zhang, H., & Chen, A. B. (2023). Transient luminous events and their relationship to lightning strokes over the Tibetan Plateau and its comparison regions. *Journal of Geophysical Research: Atmospheres*, *128*(8), e2022JD037292. <https://doi.org/10.1029/2022JD037292>
- Xu, C., & Zhang, W. (2023). The perturbation of ozone and nitrogen oxides impacted by blue jet considering the molecular diffusion. *Fluids*, *8*(6), 176. <https://doi.org/10.3390/fluids8060176>
- Yang, J., Qie, X., Zhong, L., He, Q., Lu, G., Wang, Z., et al. (2020). Analysis of a gigantic jet in southern China: Morphology, meteorology, storm evolution, lightning, and narrow bipolar events. *Journal of Geophysical Research: Atmospheres*, *125*(15), e2019JD031538. <https://doi.org/10.1029/2019JD031538>